

1 Effect of Sequence Depth and Length in Long-read

2 Assembly of the Maize Inbred NC358

3

4 Shujun Ou¹, Jianing Liu², Kapeel M. Chougule³, Arkarachai Fungtammasan⁴, Arun Seetharam⁵, Joshua
5 Stein³, Victor Llaca⁶, Nancy Manchanda¹, Amanda M. Gilbert⁷, Xuehong Wei³, Chen-Shan Chin⁴, David
6 E. Hufnagel¹, Sarah Pedersen¹, Samantha Snodgrass¹, Kevin Fengler⁶, Margaret Woodhouse⁸, Brian P.
7 Walenz⁹, Sergey Koren⁹, Adam M. Phillippy⁹, Brett Hannigan⁴, R. Kelly Dawe^{2,*}, Candice N. Hirsch^{7,*},
8 Matthew B. Hufford^{1,*}, Doreen Ware^{3,10,*}

9

10 1. Department of Ecology, Evolution, and Organismal Biology, Iowa State University, Ames, IA
11 50011, USA

12 2. Department of Genetics, University of Georgia, Athens, GA 30602, USA

13 3. Cold Spring Harbor Laboratory, Cold Spring Harbor, NY 11724, USA

14 4. DNAnexus, Inc., Mountain View, CA 94040, USA

15 5. Genome Informatics Facility, Iowa State University, Ames, IA 50011, USA

16 6. Genomics Technologies, Applied Science and Technology, Corteva AgriscienceTM, IA 50131,
17 USA

18 7. Department of Agronomy and Plant Genetics, University of Minnesota, St. Paul, MN 55108,
19 USA

20 8. USDA ARS Corn Insects and Crop Genetics Research Unit, Ames, IA 50011, USA

21 9. Genome Informatics Section, Computational and Statistical Genomics Branch, National Human
22 Genome Research Institute, National Institutes of Health, Bethesda, MD 20892, USA

23 10. USDA ARS NAA Robert W. Holley Center for Agriculture and Health, Agricultural Research
24 Service, Ithaca, NY 14853, USA

25 *To whom correspondence should be addressed: kdawe@uga.edu (RKD), cnhirsch@umn.edu (CNH),
26 mhufford@iastate.edu (MBH), or ware@cshl.edu (DW).

27

28 Abstract

29 Recent improvements in the quality and yield of long-read data and scaffolding technology have made it
30 possible to rapidly generate reference-quality assemblies for complex genomes. Still, generating these
31 assemblies is costly, and an assessment of critical sequence depth and read length to obtain high-quality
32 assemblies is important for allocating limited resources. To this end, we have generated eight independent
33 assemblies for the complex genome of the maize inbred line NC358 using PacBio datasets ranging from
34 20-75x genomic depth and N50 read lengths of 11-21 kb. Assemblies with 30x or less depth and N50 read
35 length of 11 kb were highly fragmented, with even the low-copy genic fraction of the genome showing
36 degradation at 20x depth. Distinct sequence-quality thresholds were observed for complete assembly of
37 genes, transposable elements, and highly repetitive genomic features such as telomeres, heterochromatic
38 knobs and centromeres. This study provides a useful resource allocation reference to the community as
39 long-read technologies continue to mature.

40 Main

41 During the two decades following the publication of the first larger eukaryotic genomes (i.e.,
42 *Drosophila melanogaster*¹ and *Homo sapiens*²), considerable progress has been made in sequencing
43 technology and assembly methods, improving our basic knowledge of genome complexity across the tree
44 of life. We now understand that genome composition (e.g., gene complement, the extent of intergenic
45 space, and the landscape of transposable elements (TEs)) varies substantially at both the inter- and
46 intraspecific levels. For example, comparing the *Arabidopsis thaliana*^{3,4} and bread wheat (*Triticum*
47 *aestivum*)⁵ genomes demonstrates a >100-fold difference in genome size (0.12 Gb and 14.5 Gb,
48 respectively) and substantial variation in both gene number (32,041 versus 107,891 annotated gene
49 models) and repeat content (21% versus 85%).

50 The goal of robust genome assembly is to capture and accurately represent all components of a
51 genome so their biology may be accurately studied. Next-generation assemblies initially relied on short-
52 read data due to cost and technological limitations. While these assemblies represented genes reasonably
53 well, repetitive regions containing transposable elements and tandem repeats were either omitted or
54 highly fragmented⁶. Newly developed long-read sequencing technology now enables contiguous
55 assembly of even the repetitive fraction of eukaryotic genomes⁷ with, for example, a complete telomere-
56 to-telomere human X chromosome recently being assembled⁸.

57 The cost of long-read sequence data can still be prohibitive for species with larger genomes, and
58 the critical target for average read length and read depth remains unclear. A full assessment of the impacts

59 of varying sequence read length and depth on the contiguity and completeness of assemblies is therefore
 60 essential for informed allocation of finite resources. Here we conduct a comprehensive assembly
 61 experiment using subsets of a high-depth, long-read (PacBio) data set for the maize inbred line NC358 to
 62 evaluate critical inflection points of quality during the assembly of a complex, repeat-rich genome.

63 We sequenced the NC358 genome to 75x depth (based on a ~2.27 Gb genome size⁹) using the
 64 PacBio Sequel platform, which generated a raw read N50 of 21.2 kb (**Table 1; Table S1; Figure S1**). To
 65 identify an optimal assembly approach for this study, the complete raw data from NC358 and data from
 66 the B73 v4 genome assembly (68x depth)¹⁰ were each assembled using Falcon¹¹, Canu¹², and a hybrid
 67 approach in which Falcon was used for error correction and Canu was used for assembly. All assembled
 68 contigs were superscaffolded with a *de-novo* Bionano optical map (**Figure S2**), and pseudomolecules
 69 were constructed based on maize GoldenGate genetic markers¹³ and high-density maize pan-genome
 70 markers¹⁴ (Online Methods). The Falcon-Canu hybrid assemblies of both genomes showed consistently
 71 higher quality in terms of contig length, Bionano conflicts, Benchmarking Universal Single-Copy
 72 Orthologs (BUSCOs)¹⁵, and LTR Assembly Index (LAI)⁷ (**Table S2**), thus this method was used for all
 73 subsequent assemblies performed on subsets of the data.

74

75 **Table 1.** Summary statistics for NC358 assemblies.

Experiment	21k_20x	21k_30x	21k_40x	21k_50x	21k_60x	21k_75x	11k_50x	16k_50x
Raw reads (Gb)	45.62	68.16	91.01	113.89	136.80	171.08	113.63	113.60
Raw coverage	20x	30x	40x	50x	60x	75x	50x	50x
Max read length (kb)	89.6	103.3	103.3	103.3	103.3	103.3	88.3	69.8
Raw read N25 (kb)	30.1	30.1	30.1	30.1	30.1	30.1	14.5	21.6
Raw read N50 (kb)	21.2	21.2	21.2	21.2	21.2	21.2	11.1	16.8
Corrected reads (Gb)	25.11	48.13	66.05	82.96	88.93	100.90	79.26	80.22
Corrected coverage	11x	21x	29x	37x	39x	44x	35x	35x
Corrected read N50 (kb)	18.42	17.13	17.10	17.25	18.80	20.05	10.37	14.48
Contig number	10,563	2,015	641	407	360	327	5,683	1,036
Contig total (Gb)	1.60	2.11	2.12	2.12	2.13	2.13	2.10	2.12
Longest contig (Mb)	1.06	11.50	47.89	76.00	79.68	78.40	4.37	21.45
Contig N50 (Mb)	0.18	1.82	7.48	16.27	22.12	24.54	0.56	4.24
Longest scaffold (Mb)	198.5	198.7	237.1	237.2	237.1	237.3	205.4	237.6
Scaffold N50 (Mb)	95.3	96.9	99.2	98.5	99.4	99.2	98.5	99.4
Assembled (%) ^a	70.4%	92.8%	93.3%	93.3%	93.7%	93.7%	92.4%	93.2%
Assembly gaps (%)	24.50%	0.90%	0.43%	0.34%	0.31%	0.31%	2.01%	0.48%
Effective assembly size (Gb) ^b	1.33	1.67	1.70	1.72	1.74	1.75	1.68	1.70
Optical map conflict ^c	594	125	56	31	22	21	386	107
Complete BUSCOs ^d	68.0%	95.5%	96.5%	96.4%	96.2%	96.3%	95.7%	96.7%

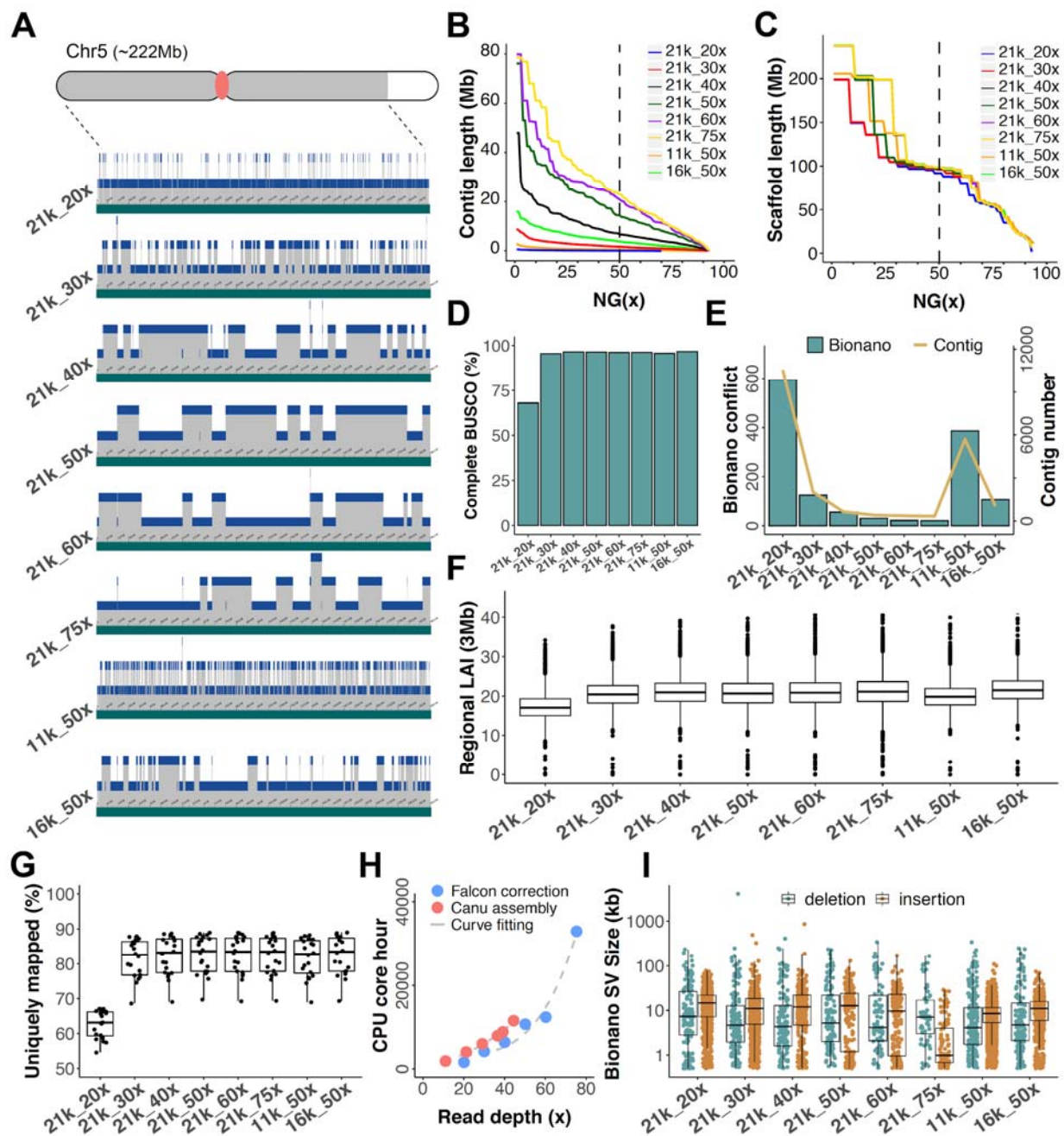
LTR Assembly Index (LAI)	12.2	19.8	20.4	20.2	20.4	20.6	19.1	21.0
Falcon CPU hour	1,563	4,162	6,363	10,693	12,386	32,950	9,721	9,224
Falcon RAM (Gb)	75	75	75	75	75	75	75	75
Canu CPU hour	1,860	4,036	5,959	7,914	8,849	11,520	6,400	7,174
Canu RAM (Gb)	61	112	149	177	201	120	183	174

76 ^aCalculated based on total contig size and the estimated genome size of 2.2724 Gb. ^bSum of unique 150-
77 mers. ^cThe optical map was generated using the Direct Label and Stain (DLS) approach with enzyme
78 DLE-1. ^dPilon-polished assemblies were used to calculate BUSCO.

79
80 Raw reads were downsampled from 75x to 60x, 50x, 40x, 30x, and 20x while maintaining a 21-
81 kb raw-read N50 and to 50x depth with a raw-read N50 of 11 kb and 16 kb. These latter two data sets
82 were generated to mirror read length distributions used in recent PacBio assemblies with similar genome
83 sizes, including the human HG002 (ref. ¹⁶) and maize B73 v4 (ref. ¹⁰) genome assemblies (**Figure S3**).
84 NC358 read subsets were error-corrected and assembled using the hybrid assembly approach described
85 above (Online Methods; Supplementary Text). These processes were resource-intensive and were
86 accelerated through cloud computing. The CPU time required for both Falcon error correction and Canu
87 assembly increased substantially as read depth increased, while the required maximum memory was fairly
88 similar (**Figure 1H; Table 1**).

89 Most assemblies had a total contig size covering >92% of the flow-cytometry estimated genome
90 size of NC358 (2.27 Gb⁹), with the notable exception of the 21k_20x assembly (70.4% covered; **Table 1**).
91 Contig length metrics were positively correlated with both read length and sequence coverage (**Figure**
92 **1B**), with the highest contig N50 (24.54 Mb) and the longest contig (79.68 Mb) observed in the 21k_75x
93 and 21k_60x assembly, respectively (**Table 1**). A dramatic drop in quality was observed for both the
94 lowest depth (21k_20x) and shortest sequence length (11k_50x) assemblies, where the number of contigs
95 was 17x - 32x more than the complete 21k_75x dataset (**Table 1; Figure 1E**).

96



97
 98 **Figure 1.** Assembly of NC58 using various read lengths and coverage. (A) Hybrid scaffolding using the
 99 Bionano optical map. A 199-Mb scaffold from chromosome 5 is shown. Grey areas on the chromosome
 100 cartoon represent the 199-Mb scaffold; the white area is the remaining 23-Mb scaffold in chromosome 5;
 101 the red dot is the centromere. Green tracts represent scaffolded sequences, and blue tracts show the
 102 contigs that comprise this scaffold with contigs jittered across three levels. (B) Contig NG(x). (C)
 103 Scaffold NG(x). (D) BUSCO. (E) The number of conflicts between Bionano contigs and sequence contigs
 104 and the number of contigs of each assembly. (F) Regional LAI values estimated based on 3-Mb windows

105 with 300-kb steps. (G) Unique mapping rate of RNA-seq libraries. Each dot represents an RNA-seq
106 library. (H) CPU core hours required for Falcon correction and Canu assembly. (I) Bionano optical map
107 inconsistency. Deletions and insertions are cases where sequences are shorter or longer than the size
108 estimated by the optical map, respectively.

109
110 For each assembly, superscaffolds were generated from the contigs using a common Bionano
111 optical map. Even the most fragmented Falcon-Canu assembly could be scaffolded to high contiguity
112 using this optical map due to the high density of labels in the map (**Figure 1A-C**). The resulting
113 assemblies all had scaffold N50s at ~98 Mb (**Table 1**). In fact, chromosome 3 (~237 Mb) consisted of a
114 single scaffold in five out of eight assemblies (**Table 1**). However, conflicts versus the Bionano map were
115 much higher in the assemblies with 20x coverage and a raw-read N50 of 11 kb (**Table 1; Figure 1E**),
116 suggesting assembly error increased with lower coverage and read length. Assemblies with shorter read
117 length contained many more deletions relative to the optical map (**Figure 1I**), which may be due to the
118 collapse of repetitive sequences. We did not observe a clear pattern between read length and deletion size
119 (**Figure 1I**). Assembly misjoins were reduced with both longer reads and higher coverage, as shown by
120 the relative number of insertions (**Figure 1I**).

121 For each of the assemblies, pseudomolecules were constructed using the GoldenGate and pan-
122 genome genetic markers, which placed >99% of the total assembled bases into pseudomolecules (**Table**
123 **S3; Figure S4**). The resulting NC358 pseudomolecules were highly syntenic across assemblies and to the
124 B73 v4 genome (**Figure S5**).

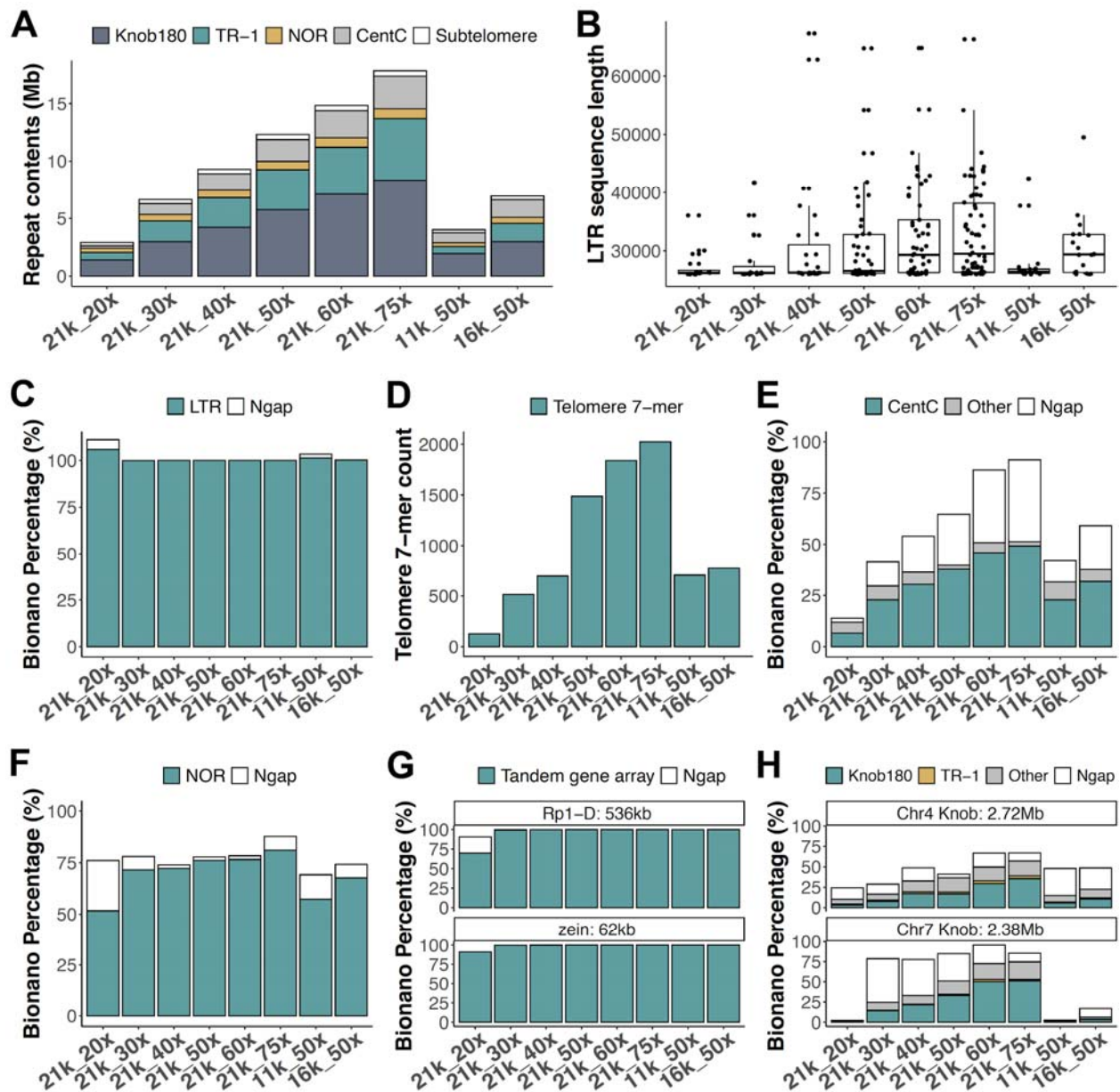
125 We evaluated the completeness of gene-rich regions in each of the assemblies using BUSCO¹⁵.
126 The percentage of complete BUSCO genes increased from 68.0% to 96.3% from the 21k_20x to the
127 21k_75x assembly (**Table 1; Figure 1D; Table S4**). Minimal improvement in BUSCO scores was
128 achieved at depths higher than 30x (95.5% complete BUSCO genes), indicating this depth provides
129 satisfactory gene space assembly.

130 To further evaluate the assembly of genic regions, we annotated gene models in the 21k_20x and
131 the 21k_75x assemblies (Online Methods) and obtained a total of 28,275 and 39,578 genes, respectively
132 (**Table S5**), with 92% of missing genes in the 21k_20x assembly falling within sequence gaps (**Table 1**).
133 Exon and intron lengths of the annotated genes were similar across the assemblies (**Table S5**).
134 Additionally, we sequenced RNA libraries from 10 tissues with two biological replicates (Online
135 Methods). On average, 80% of reads in these libraries could be uniquely mapped to the various NC358
136 assemblies (**Figure 1G**). The 21k_20x assembly was a notable exception with only 63% of reads
137 uniquely mapped (**Figure 1G; Figure S6**). We extracted the reads that did not map to the 21k_20x
138 assembly and remapped them to the 21k_75x assembly, obtaining a unique-mapping rate of 36% (**Table**

139 **S6**). These reads mapped to 3,184 genes in the 21k_75x assembly (**Table S7**). Of these 3,184 genes, 20%
 140 are present in the 21k_20x assembly but had assembly errors that prevented the RNA-seq reads from
 141 mapping, while the other 80% were within sequence gaps (**Table S7**).

142 In addition to metrics of gene completeness, we also examined each assembly for its ability to
 143 capture two notable maize tandem gene arrays, *Rp1-D*¹⁷ and *zein*¹⁸. The total length of these gene arrays
 144 was estimated at 536 kb and 62 kb in NC358 respectively based on the optical map. Both the *Rp1-D* and
 145 *zein* loci were completely assembled in all except for the 21k_20x assembly, where only 70% and 91% of
 146 the loci were assembled respectively (**Figure 2G**; **Table S8**).

147



148

149 **Figure 2.** Assembly of repetitive components in the NC358 genome. (A) The assembled size of the 180-
150 bp knob repeat, the knob TR-1 element, the chromosome 6 NOR region, CentC arrays, and subtelomere
151 arrays in each of the NC358 assemblies. (B) Length distribution of LTR retrotransposons longer than 26
152 kb. Each dot represents an annotated sequence. (D) Telomere 7-mer counts in telomere regions of NC358
153 assemblies. Assembly of (C) LTR retrotransposons, (E) CentC arrays, (F) the chromosome 6 NOR region,
154 (G) the *Rp1-D* and *zein* tandem gene arrays, and (H) two example knobs in each of the NC358 assemblies.
155 The NC358 Bionano optical map was used to estimate the size of these components. Ngap, estimated gap
156 size.

157

158 The completeness of transposon-rich regions of the genome was assessed through the assembly
159 index of LTR retrotransposons, called LAI⁷. A higher LAI score is indicative of a more complete
160 assembly in TE-rich regions. The 21k_20x assembly had a substantially lower LAI score compared to
161 other assemblies (LAI = 12.2; **Table 1**). As sequence depth increased a substantial improvement in LAI
162 was observed, while the effect of sequence length on LAI was minimal (**Figure 1F**). This is likely due to
163 the fact that the length of LTR retrotransposons is approximately 10 kb on average (**Figure S7**), which
164 could be spanned by even the 11 kb reads. The assemblies that were generated from $\geq 40x$ genomic depth
165 achieved “gold” quality (LAI ≥ 20 (ref. ⁷)) (**Table 1; Figure 1F**), which was comparable to the B73 v4
166 genome and much higher than many previously published maize genome assemblies generated with
167 short-read data (**Figure S8**).

168 The insertion time of each LTR retrotransposon can be dated based on sequence divergence
169 between terminal repeats⁷. We identified 36% fewer intact LTR retrotransposons in the highly fragmented
170 21k_20x assembly (**Figure S9**), and significantly older LTR elements in the 11k_50x assembly ($p < 10^{-5}$,
171 Tukey's test), suggesting fragmentation of assemblies could bias conclusions of transposon studies. LTR
172 retrotransposons shorter than 26 kb were assembled well across the assemblies (**Figure S10; Figure S11**).
173 However, a substantial effect of longer reads and higher depth was observed in the assembly of LTR
174 sequences longer than 26 kb (**Figure 2B**). We examined the assemblies of the longest LTR sequence
175 clusters using the Bionano optical map and found most assemblies contained no gaps and were virtually
176 complete (**Figure 2C**), with the notable exception that the 11k_50x, 16k_50x, and 21k_20x assemblies,
177 which contained large gaps in one of the LTR clusters (**Table S9**). We also inspected the *bz* locus¹⁹,
178 which has highly nested transposon insertions and an estimated size of 303.5 kb in NC358. The *bz* locus
179 was well assembled in all but the 21k_20x assembly, in which only 56.3% of the sequence was included
180 (**Table S10**). In summary, with $\geq 40x$ of sequence coverage, long-read sequencing and assembly can
181 traverse most transposon-rich genomic regions including relatively long LTR sequences, though with
182 shorter reads (*i.e.*, read N50 of 11 kb - 16 kb) this sequencing depth may not be sufficient.

183 The assembly of non-TE tandem repeat space was also evaluated, including telomeres (7-bp
184 repeats), subtelomeres (300 - 1300-bp repeats), CentC arrays (156-bp repeats), nucleolus organizer region
185 (NOR, ~11 kb repeats), and the two major knob repeats (mixture of 180-bp and 350-bp repeats) (**Figure**
186 **2A; Table S11**). The effects of sequence read depth and sequence read length were far more pronounced
187 across many of these tandemly duplicated portions of the genome (**Figure 2A**).

188 Telomeres are characterized by 7-bp tandem repeats at the end of each chromosome. Our results
189 showed a substantial increase in the assembled length of telomere sequence with the increase of both read
190 length and sequence coverage (**Figure 2D; Table S12**). However, a precise estimate of telomere length
191 was not possible with our optical map due to the lack of Bionano DLE-1 sites in these highly repetitive
192 regions. Using the full dataset (21k_75x), only 10 of 20 telomere-subtelomere combined regions were
193 assembled to >90% of the Bionano estimated size (**Table S13**), suggesting even longer reads and higher
194 coverage are required for the full assembly of these regions.

195 The centromere is one of the most repetitive regions of many species' genomes including maize.
196 We characterized NC358 centromeres based on CentC arrays²⁰ which are abundant in functional
197 centromeric regions²¹. Even with the full dataset (21k_75x), only half of CentC arrays were assembled
198 (**Figure 2E; Figure S12; Table S14**). Hybrid scaffolded assemblies with sequence coverage $\geq 60x$
199 yielded a better approximation to the Bionano estimated size, even though these regions largely consisted
200 of gaps (**Figure 2E**). Although assembled sequences were not significantly increased, higher sequence
201 depth resulted in better anchoring of sequences with the Bionano optical map. Only three centromeres,
202 which contained a mixture of CentC arrays, transposons, and intergenic sequences, could be traversed by
203 Bionano DLE-1 labeling due to having a comparatively higher content of low-copy sequence²¹. The size
204 of the remaining centromeres was likely underestimated (**Figure S13**), and further improvements in
205 scaffolding technology are required to traversing these regions.

206 The NOR is enriched with ribosomal DNA (rDNA) and spans approximately 9 Mb on
207 chromosome 6 of NC358 (**Table S15**). Longer read length improved the assembly of this region, but
208 substantial differences were not observed with coverage $\geq 30x$ (**Figure 2F**). Approximately 72% of the
209 NOR was included in the 21k_30x assembly and this improved by just 9% to 81% in the 21k_75x
210 assembly (**Table S15; Figure 2F**).

211 Finally, maize knobs are heterochromatic regions consisting of 180-bp (knob180) and 350-bp
212 (TR-1) repeats²². We used the Bionano optical map to assess the assembly of two knobs that together
213 spanned a total of 5 Mb. With longer reads and higher coverage, more knob sequences were assembled,
214 with 6.5% of the two knobs present in the 21k_20x assembly and up to 65% in the 21k_75x assembly
215 (**Table S16; Figure 2H**).

216 Recent innovations in long-read and scaffolding technology have made highly contiguous
217 assembly possible across a wide range of species. We have documented how both the completeness and
218 contiguity of assemblies improve with increasing depth and read length. The biological aims of an
219 investigation must be considered when determining the level of investment in depth of sequence. With
220 long-read sequencing, the low-copy gene space (including tandem gene arrays) can be well assembled
221 with as low as 30x genomic coverage across a range of read lengths. Complete characterization of
222 transposable elements in complex genomes such as maize will require a greater depth of sequence (~40x)
223 and should employ library preparation protocols that maximize read-length N50. Finally, complete
224 assembly of highly repetitive genomic features such as heterochromatic knobs, telomeres, and
225 centromeres will require substantially more data. In fact, complete assembly of these latter highly
226 repetitive sequences will likely require innovations beyond current sequencing technology.

227 ONLINE METHODS

228 Sample preparation

229 Seeds for the maize NC358 inbred line were obtained from GRIN Global (seed stock ID Ames
230 27175), grown, and self-pollinated at Iowa State University in 2017. A total of 144 seedlings derived
231 from a single selfed ear were grown in the greenhouse. Leaf tissues from the seedlings at the Vegetative 2
232 (V2) growth stage were sampled after a 48-hour dark treatment to reduce carbohydrates. A total of 35g of
233 tissue was harvested and flash-frozen. Tissue was sent to the Arizona Genomics Institute (AGI) for high
234 molecular weight DNA isolation using a CTAB protocol²³.

235 Illumina and PacBio Sequencing

236 Pacific BioSciences long-read data for NC358 were generated at AGI using the Sequel platform.
237 Libraries were prepared using the manufacturer's suggested protocol (<https://www.pacb.com/>). The raw
238 reads that were generated covered the genome at an estimated 75-fold depth (75x) with a read-length N50
239 of 21,166 bp. Reads from each SMRT cell were inspected and quality metrics were calculated using
240 SequelQC²⁴. After validating the PSR (polymerase to subread ratio) and ZOR (ZMW occupancy ratio)
241 were satisfactory, all subreads were used for subsequent steps.

242 Paired-end Illumina data for NC358 were generated at the Georgia Genomics and Bioinformatics
243 Core (GGBC) from the same DNA extraction as was used for the long-read sequencing. Quality control
244 of DNA was conducted using Qubit and Fragment Analyzer to determine the concentration and size
245 distribution of the DNA. The library was constructed using the KAPA Hyper Prep Kit (Cat# KK8504).

246 During library preparation, DNA was fragmented by acoustic shearing with Covaris before end repair and
247 A-tailing. Barcoded adaptors were ligated to DNA fragments to form the final sequencing library.
248 Libraries were purified and cleaned with SPRI beads before being amplified with PCR. Final libraries
249 underwent another bead cleanup before being evaluated by Qubit, qPCR (KAPA Library Quantification
250 Kit Cat# KK4854), and Fragment Analyzer. The final pool undergoing Illumina's Dilute and Denature
251 Libraries protocol was diluted to 2.2 pM for loading onto the sequencer and then sequenced with 1%
252 PhiX by volume. Libraries were sequenced on the NextSeq 500 instrument using PE150 cycles. The
253 demultiplexing was done on Illumina's BaseSpace.

254 PacBio SMRT subreads for the maize inbred line B73 (sequenced to 68x depth) were retrieved
255 from the NCBI SRA database with accession ID SRX1472849 (ref. ¹⁰). PacBio SMRT subreads for the
256 human HG002 sample (sequenced to 147x depth) were retrieved with accession IDs SRX1033793 and
257 SRX1033794 (ref. ¹⁶).

258 Downsampling raw sequence

259 The 75x SMRT Sequel raw data from maize NC358 was downsampled to 60x, 50x, 40x, 30x, and
260 20x data using seqtk (v1.2) (<https://github.com/lh3/seqtk>). Downsampling was performed as serial
261 titration, in which each dataset was the superset of the next smaller dataset, and was sampled to have
262 similar length distributions (**Figure S3**). The N50 of the downsampled raw data were almost identical to
263 the N50 of the full 75x data (**Table 1**).

264 Shifting read length distribution of raw sequence

265 Two more NC358 datasets were downsampled and trimmed from the original 75x SMRT dataset
266 to match the read length distribution of the maize B73 data¹⁰ and the human HG002 data¹⁶, which had
267 read N50 lengths of ~16 kb and ~11 kb, respectively (**Figure S3**). To do this, first, the read lengths of the
268 maize B73 and human HG002 data were each sorted in descending order. For each read length value, all
269 raw reads from NC358 that were longer than said value were randomly sampled without replacement and
270 clipped to have matched read length. The unused clipped part of the read was put back in the pool for
271 further use with short read length. This distribution-shifting approach was chosen to achieve a realistic
272 distribution of read length rather than trimming all reads by fixed lengths. These datasets were labeled as
273 "16k", and "11k" based on their N50 of raw data of 16,765, and 11,092, respectively.

274 RNA tissue sampling and sequencing

275 Samples from 10 tissues throughout development were collected to generate expression evidence
276 for gene annotation. Two biological replicates were collected for each tissue type, and each replicate
277 consisted of three individual plants. The tissues that were sampled were: 1) primary root at six days after
278 planting; 2) shoot and coleoptile at six days after planting; 3) base of the 10th leaf at the Vegetative 11
279 (V11) growth stage; 4) middle of the 10th leaf at the V11 growth stage; 5) tip of the 10th leaf at the V11
280 growth stage; 6) meiotic tassel at the Vegetative 18 (V18) growth stage; 7) immature ear at the V18
281 growth stage; 8) anthers at the Reproductive 1 (R1) growth stage; 9) endosperm at 16 days after
282 pollination; and 10) embryo at 16 days after pollination. Tissue from developmental stage V11 and older
283 were taken from field-grown plants while all younger tissue samples were taken from greenhouse-grown
284 plants. For the endosperm and embryo samples, tissue from 50 kernels per plant (150 total per biological
285 replicate) were sampled. Greenhouse-grown plants were planted in Metro-Mix300 (Sun Gro Horticulture)
286 with no additional fertilizer and grown under greenhouse conditions (27°C/24°C day/night and 16h/8h
287 light/dark) at the University of Minnesota Plant Growth Facilities. Field grown plants were planted at the
288 Minnesota Agricultural Experiment Station located in Saint Paul, MN with 30-inch row spacing at
289 ~52,000 plants per hectare. RNA was extracted using the Qiagen RNeasy plant mini kit following the
290 manufacturer's suggested protocol.

291 The quality of the total RNA was assessed by Bioanalyzer or Fragment analyzer to determine
292 RNA concentration and integrity. The sample concentration was normalized in 25 uL of nuclease-free
293 H₂O before library preparation. Libraries were prepared using KAPA's stranded mRNA-seq kit with
294 halved reaction volumes. During library preparations, mRNA was selected using oligo-dT beads, the
295 RNA was fragmented, and cDNA was generated using random hexamer priming. Single or dual indices
296 were ligated depending on the desired level of multiplexing. The number of cycles for library PCR was
297 determined based on kit recommendations for the amount of total RNA used during library preparation.
298 Libraries were quality control checked using Qubit or plate reader, depending on the number of samples
299 in the batch for library concentration, and fragment analyzer for the size distribution of the library. The
300 pooling of samples was based on qPCR. The pooled libraries were then checked by Qubit, Fragment
301 Analyzer, and qPCR.

302 RNA libraries were prepared for sequencing on Illumina instruments using Illumina's Dilute and
303 Denature protocol. Pooled libraries were diluted to 4 nM, then denatured using NaOH. The denatured
304 library was further diluted to 2.2 pM, and PhiX was added at 1% of the library volume. RNA pools were
305 sequenced on a NextSeq 550 to generate 75 bp pair-end reads. On average, 24.5 million pair-end reads
306 were generated per replicate per tissue type, for a total of 489 million reads across all samples. Data were
307 demultiplexed and trimmed of adapter and barcode sequences on BaseSpace (**Figure S14**).

308 Bionano data generation

309 The DNA extraction was performed using the Bionano Prep™ Plant Tissue DNA Isolation Kit
310 according to a modified version of the Plant Tissue DNA Isolation Base Protocol. Approximately 0.5g
311 leaf tissue was collected from young etiolated seedlings germinated in soil-free conditions and grown in
312 the dark for approximately two weeks after germination. Freshly-cut leaves were treated with a 2%
313 formaldehyde fixing solution and then washed, cut into small pieces and homogenized using a Qiagen
314 TissueRuptor probe. Free nuclei were concentrated by centrifugation at 2000 xg, washed, isolated by
315 gradient centrifugation and embedded into a low-melting-point agarose plug. After proteinase K and
316 RNase A treatments, the agarose plug was washed four times in Wash Buffer and five times in TE (Tris
317 and EDTA) buffer. Finally, purified ultra-high molecular weight nuclear DNA (uHMW nDNA) was
318 recovered by melting the plug, digesting it with agarase and subjecting the resulting sample to drop
319 dialysis against TE.

320 The Bionano Saphyr platform, in combination with the Direct Label and Stain (DLS) process,
321 was used to generate chromosome-level sequence scaffolds and validate PacBio sequence contigs. Direct
322 labeling was performed using the Direct Labeling and Staining Kit (Bionano Genomics Catalog 80005)
323 according to the manufacturer's recommendations, with some modifications²⁵. In total, 1 ug uHMW
324 nDNA was incubated for 2:20 h at 37 °C, followed by 20 min at 70 °C in the presence of DLE-1 Enzyme,
325 DL-Green and DLE-1 Buffer. Following proteinase K digestion and cleanup of the unincorporated DL-
326 Green label, the labeled DNA was combined with Flow Buffer, DTT, and incubated overnight at 4 °C.
327 DNA was quantified and stained by adding Bionano DNA Stain to a final concentration of 1 microliter
328 per 0.1 microgram of final DNA. The labeled sample was loaded onto a Bionano chip flow cell and
329 molecules separated, imaged and digitized in a Bionano Genomics Saphyr System and server according to
330 the manufacturer's recommendations (<https://bionanogenomics.com/support-page/saphyr-system/>).

331 Data visualization, processing, DLS map assembly, and hybrid scaffold construction were all
332 performed using the Bionano Genomics software Access, Solve, and Tools. A filtered subset of 1,282,746
333 molecules (353,596 Mb total length) with a minimum size of 150 kb and a maximum size of 3 Mb were
334 assembled without pre-assembly using the non-haplotype parameters with no CMPR cut and without
335 extend-split.

336 Genome assembly

337 To determine the assembly approach to apply to each of the datasets, three different methods
338 were first tested on the complete dataset, including Falcon only, Canu only, and a Falcon-Canu hybrid

339 approach. We also downloaded raw PacBio sequencing data for the B73 v4 genome for comparison of the
340 different approaches with a second data set.

341 The Falcon genome assemblies were performed using the falcon_kit pipeline v0.7 (ref. ¹¹) with
342 some modifications. TANmask and REPmask were not used due to their extensive masking for the maize
343 genome. Error correction for raw reads was performed on the longest 50x coverage, with the average read
344 correction rate set to 75% (-e 0.75) and local alignments for at least 3000 bp (-l 3000). The usage of -l
345 3000 instead of -l 2500 was done because of the omitted repeat masking, which works better for highly
346 repetitive genome species like maize. A minimum of two reads and a maximum of 200 reads were used
347 for error corrections (--min_cov 2 --max_n_read 200). For sequence assembly, the exact matching k-mers
348 between two reads was set to 24 bp (-k 24) with read correction rate as 95% (-e 0.95) and local
349 alignments at least 1000 bp (-l 1000). The longest 20x coverage reads were used for assembly with a
350 minimum coverage of two and maximum coverage of 80 (--min_cov 2 --max_cov 80). Full parameter sets
351 are included in the supplementary text.

352 For Canu read correction and assembly, Canu v1.7 (ref. ¹²) was used. K-mers more frequent than
353 500 were not used to seed overlaps (ovlMerThreshold=500). The genome size of 2,272,400,000 bp and
354 2,500,000,000 bp for NC358 and B73, respectively, were used in this study⁹. Other parameters were used
355 as default. Due to a bug in the Canu v1.7 program, truncations of large contigs would occur during the
356 consensus process (<https://github.com/marbl/canu/releases/tag/v1.8>). Because the program was not
357 expecting the superlong contigs that were being generated for our NC358 assemblies, we found a total of
358 nine large contigs that suffered from consensus truncations. To fix these truncation gaps, consensus-free
359 contigs were generated using Canu v1.7 (cnsConsensus=quick), then blastn was used to search for 5-kb
360 boundaries of truncation gaps in consensus-free assemblies. Truncated sequences were retrieved and
361 patched to the truncated contigs.

362 For the Falcon-Canu hybrid approach, the error correction was performed by Falcon, and the
363 trimming and assembly were performed by Canu using the versions and parameters described above. All
364 the assemblies were performed on the DNAnexus cloud platform. CPU core hour and maximum memory
365 usage were recorded every 10 minutes for each Falcon error correction and Canu assembly job. For
366 Falcon error correction of the 21k datasets, the CPU core hour (y) could be predicted by raw read depth
367 (m) with $y = 20603100000 + (3136.685 - 20603100000)/(1 + (m/1932.377)^{4.148144})$. For Canu
368 assembly of the 21k datasets, the CPU core hour (y) could be predicted by corrected read depth (n) with
369 $y = 6438752000 + (1284.689 - 6438752000)/(1 + (n/56334.74)^{1.872455})$. These curves were fit using the
370 <https://mycurvefit.com/> website and plotted in R.

371 We evaluated these assembly approaches using both maize NC358 and B73. For both inbred lines,
372 a similar assembly size was generated by each of the approaches. However, the Falcon-Canu hybrid

373 approach yielded the longest contig length (78.4 Mb and 19.7 Mb, respectively), the highest contig NG50
374 (23.0 Mb and 3.0 Mb, respectively), and the lowest number of assembly errors based on Bionano conflict
375 cuts (21 and 64, respectively; **Table S1**). The gene space completeness evaluated using Benchmarking
376 Universal Single-Copy Orthologs (BUSCOs)¹⁵ and the repeat space continuity evaluated using the LTR
377 Assembly Index (LAI) (vbeta3.2)⁷ were similar between the Canu and the hybrid approach and higher
378 than those assemblies that were created using the Falcon assembler (**Table S1**). This was likely due to the
379 consensus approach used at the end of the Canu program, which was missing in the Falcon program. Due
380 to the consistently high quality of the assemblies generated from the hybrid approach, we used this
381 approach to assemble each of the NC358 datasets with varying sequence depth and read length. Full
382 parameter sets are included in the supplementary text.

383 Genome polishing

384 Two polishing approaches were tested on the 21k_75x assembly. The first was done using Arrow
385 with PacBio raw reads (75x coverage). Read mapping to the assembly was done using BLASR²⁶ with
386 default parameters (--minMatch 12 --bestn 10 --minPctSimilarity 70.0 --refineConcordantAlignments).
387 The Arrow tool in the SMRT Link (v5.1.0) software package was then applied to correct for sequencing
388 errors with default parameters. A second approach for polishing was done using Pilon with Illumina pair-
389 end reads (30.7x coverage). Read mapping to the assembly was done using Minimap2 (v2.16)²⁷ with the
390 short read option (-ax sr). Pilon (v1.23-0)²⁸ was then applied to correct for sequencing errors including
391 SNPs and small indels (--fix bases) on sites with a minimum depth of 10 and a minimum mapping quality
392 of 30 (--mindepth 10 --minmq 30).

393 With both approaches, minimal differences were observed in the contiguity statistics (**Table S2**)
394 or the repeat content for the 21k_75x assembly (**Figure S15**), and it is expected that this minimal impact
395 would be observed across all of the NC358 assemblies. A more substantial difference in BUSCO scores
396 were observed with both the Arrow-polished and the Pilon-polished 21k_75x assemblies (**Table S2**).
397 Because the polishing had a substantial impact on this metric, the other NC358 assemblies were also
398 polished using Pilon with the same parameter settings and similar improvement of BUSCO scores were
399 observed (**Table 1**; **Table S4**).

400 Generation of pseudomolecules

401 Hybrid scaffolds for the assemblies were generated with Bionano Direct Label and Stain data
402 using Bionano Solve (v3.2.1_04122018). Overlaps of contigs within Bionano map space were resolved
403 by placing 13 bp of Ns (13N gaps) at the overlap site. In addition to arranging contigs into scaffolds, the

404 hybrid scaffold was also used to detect misassembly and to assess completeness of the assembled genome
405 and repeat elements.

406 The pseudomolecules were constructed from the hybrid scaffolds using ALLMAPS (v0.8.12)²⁹.
407 Both pan-genome anchor markers¹⁴ and GoldenGate markers¹³ were used with equal weights for ordering
408 and orientating the scaffolds. For pan-genome anchor markers, data were downloaded from the CyVerse
409 Data Commons
410 (http://datacommons.cyverse.org/browse/iplant/home/shared/panzea/genotypes/GBS/v27/Lu_2015_NatC
411 [ommun_panGenomeAnchors20150219.txt.gz](http://datacommons.cyverse.org/browse/iplant/home/shared/panzea/genotypes/GBS/v27/Lu_2015_NatC)) and a bed file with 50 bp upstream and downstream of the
412 B73 v3 coordinates were generated. A text file with marker name and predicted distance was also
413 constructed from the same file. The extracted markers were mapped to HiSat2 (v2.1.0)³⁰ indexed
414 assemblies of NC358 by disabling splicing (--no-spliced-alignment) and forcing global alignment (--end-
415 to-end). Very high read and reference gap open and extension penalties (--rdg 10000,10000 and --rfg
416 10000,10000) were also used to ensure full-length mapping of marker sequence. The final alignment was
417 then filtered for mapping quality of greater than 30 and tag XM:0 (unique mapping) to retain only high-
418 quality uniquely mapped marker sequences. The mapped markers were merged with the predicted
419 distance information to generate a CSV input file for ALLMAPS. Only scaffolds with more than 20
420 uniquely mapped markers, with a maximum of 100 markers per scaffold, were used for pseudomolecule
421 construction.

422 The GoldenGate markers were downloaded from MaizeGDB
423 (https://www.maizegdb.org/data_center/map?id=1203673). For the markers with coordinates, 50 bp
424 flanking regions were extracted from the B73 v4 genome. For markers without coordinates, marker
425 sequences were used as-is, and those missing both coordinates and sequences were discarded. Mapping of
426 the markers was done similar to the method described above for the pan-genome anchor markers, with all
427 uniquely mapped markers retained. The genetic distance information for these markers was converted to a
428 CSV file before using it in ALLMAPS. ALLMAPS was run with default options, and the
429 pseudomolecules were finalized after inspecting the marker placement plot and the scaffold directions.
430 Synteny dotplots were generated using the scaffolds as well as pseudomolecule assemblies against the
431 B73 genome by following the ISUgenomics Bioinformatics Workbook
432 (<https://bioinformaticsworkbook.org/dataWrangling/genome-dotplots.html>)³¹. Briefly, the repeats were
433 masked using RepeatMasker (v4.0.9)³² and the Maize TE Consortium (MTEC) curated library³³.
434 RepeatMasker was configured to use the NCBI engine (rmbblastn) with a quick search option (-q) and GFF
435 as a preferred output. The repeat-masked genomes were then aligned using Minimap2 (v2.2)²⁷ and set to
436 break at 5% divergence (-x asm5). The paf files were filtered to eliminate alignments less than 1 kb and
437 dotplots were generated using the R package dotPlotly (<https://github.com/tpoorten/dotPlotly>).

438 Gene annotation and RNA-seq mapping

439 The MAKER-P pipeline³⁴ was used to annotate protein-coding genes for Pilon-polished NC358
440 21k_20x and 21k_75x genome assemblies. The baseline evidence used in annotating the B73 v4
441 genome¹⁰ was applied. Before gene annotation, the MTEC curated TE library³³ and RepeatMasker was
442 used to mask repetitive sequences. For gene prediction, we used Augustus³⁵ and FGENESH³⁶
443 (<http://www.softberry.com/berry.phtml>) with training sets based on maize and monocots, respectively. To
444 identify genes that were missing in the 21k_20x assembly, total coding sequences (CDS) from the
445 21k_75x annotation was masked by total CDS from the 21k_20x annotation using Repeatmasker (-div 2 -
446 cutoff 1000 -q -no_is -norma -nolow). The 21k_75x CDS that were masked less than 20% were
447 determined missing in the 21k_20x annotation. These missing CDS were blast against the 21k_20x
448 assembly and those that had less than 20% similarity were also determined to be missing in the 21k_20x
449 assembly.

450 A total of 20 RNA-seq libraries were sequenced from NC358 tissue samples. Each library was
451 sequenced to 21.9x ± 0.7x coverage with a mapping rate of 86.4% ± 1.0% to the B73 v4 using STAR
452 (v2.5.2b)³⁷ (**Figure S16; Table S17**). To benchmark the gene space assembly, STAR (v2.5.2b)³⁷ was used
453 to map the RNA-seq reads against the Pilon-polished NC358 assemblies. Unmapped reads from the
454 21k_20x assembly were extracted using SAMtools³⁸ and remapped to the 21k_75x assembly with STAR.
455 Genes with read coverage ≥20% were extracted using BEDtools³⁹, and blast against the 21k_20x
456 assembly for the identification of full-length copies. The NC358 TE library (see next section for details
457 on library generation) was used to identify TE fragments in genes with aligned reads (**Table S7**). In
458 addition, TESorter (v1.1.4)⁴⁰ (<https://github.com/zhangrengang/TEsorter>) was used to identify TE-related
459 protein domains in genes with default parameters (**Table S7**).

460 Assessment of genome assembly quality

461 The quality of the different NC358 assemblies was assessed on the unpolished assemblies unless
462 noted. For continuity, N50, NG50, NG(x), the number of contigs, and maximum contig length were
463 estimated. NG(x) values were the length of the contig at the top x percent of the estimated genome size
464 (2.2724 Gb) consisting of the longest contigs. NG50 is a commonly used case of NG(x) values. NG(x)
465 values were calculated using GenomeQC (<https://github.com/HuffordLab/GenomeQC>)⁴¹. The gene space
466 completeness was estimated using BUSCO (v3.0.2)¹⁵ with the Embryophyta odb9 dataset (n = 1,440) and
467 BLAST (v2.6)⁴², Augustus (v3.3)³⁵, EMBOSS (v6.6.0)⁴³, and HMMER (v3.1b2)⁴⁴.

468 The repeat space contiguity was assessed using the LTR Assembly Index (LAI) (vbeta3.2)⁷. To
469 annotate LTR retrotransposons, LTR_retriever (v2.6)⁴⁵ was used to identify intact LTR retrotransposons

470 and construct LTR libraries for each NC358 assembly with default parameters. To generate a high-quality
471 LTR library for NC358, assembly-specific LTR libraries were aggregated and masked by the MTEC
472 curated LTR library using RepeatMasker (v4.0.7)³². Library sequences masked over 90% were removed
473 and redundant sequences were also removed using utility scripts (cleanup_tandem.pl and
474 cleanup_tandem.pl) from the EDTA package⁴⁶. Non-redundant NC358-specific LTR sequences were
475 added to the MTEC curated LTR library to form the final LTR library for NC358. The final library was
476 then used to mask the 21k_75x assembly for the estimation of total LTR content. The total LTR content
477 of 76.34% and LTR identity of 94.854% was used to estimate LAI values of all NC358 assemblies (-
478 totLTR 76.34 -iden 94.854). The LAI of the other maize line genomes, including PH207 (GeneBank
479 Accession: GCA_002237485.1)⁴⁷, CML247 (GeneBank Accession: GCA_002682915.2)¹⁴, Mo17 (From
480 Xin *et al.* (2013)⁴⁸ and GeneBank Accession: GCA_003185045.1 (ref. ⁴⁹)), W22 (GeneBank Accession:
481 GCA_001644905.2)⁵⁰, and B73 v4 (GeneBank Accession: GCA_000005005.6)¹⁰ were also evaluated for
482 context.

483 Effective assembly size, which is the length of the uniquely mappable sequences of an assembly,
484 was estimated using unique 150-mers in each sequence assembly and quantified using Jellyfish (v2.0)⁵¹
485 with default parameters.

486 Misassembly identification with optical maps

487 The Bionano optical mapping was used as an orthogonal method to identify misassemblies in
488 genomes. Bionano *de novo* assembled optical maps were aligned to the sequence pseudomolecules to
489 characterize structural inconsistencies using the structural variant calling pipeline of BionanoSolve 3.4.
490 Default parameters were employed from the nonhaplotype_noES_DLE file. Homozygous calls with a
491 confidence of 0.1, a size of 500 bp, and non-overlaps with gap regions were regarded as insertions and
492 deletions in sequence assemblies.

493 Assembly quality evaluation in repeat space

494 The coordinates of CentC arrays, knob180, TR-1 knobs, and NOR in the assemblies were
495 identified by blasting CentC, knob180, TR-1 knob consensus sequences²¹, and the rDNA intergenic
496 spacer (AF013103.1) against each assembly. An individual repeat array was defined as clusters of
497 repetitive sequences that had less than 100 kb interspace between repeated elements. The level of repeats
498 and gaps were then quantified in each defined repeat array. Respective sizes of each repeat array in the
499 Bionano maps were estimated using the Bionano labels closest to the start and end coordinates in the
500 assemblies.

501 To identify the telomere-subtelomere boundaries of the NC358 assemblies, seven maize
502 subtelomere repeat sequences were downloaded from NCBI (EU253568.1, S46927.1, S46926.1,
503 S46925.1, CL569186.1, AF020266.1, and AF020265.1) and used as queries to blast against the NC358
504 21k_75x assembly. Subtelomere boundaries were first identified at the start and end of chromosomes
505 where blast hits were clustering then cross-checked with subtelomere-specific Fluorescence in situ
506 hybridization (FISH) data⁵². The blast results were concordant with FISH results, showing the beginning
507 of chromosomes 7, 8, 9, and 10 lack subtelomeres (**Table S13**). Telomeres were defined as the distance
508 between the boundary of subtelomeres to the end of pseudomolecules of the 21k_75x assembly, which
509 were used as the basis for estimating the telomere size and count of the telomeric repeat sequences (5'-
510 TTTAGGG-3' and 5'-CCCTAAA-3' in reverse complementation) in all other NC358 assemblies.

511 To identify the *bz* locus in the NC358 assemblies, the sequence of the maize W22 *bz* locus was
512 first downloaded from NCBI (EU338354.1)¹⁹. The starting and ending 2 kb of the W22 *bz* locus were
513 used to blast against the NC358 21k_75x assembly and the longest matches on chromosome 9 were used
514 as the location of the *bz* locus in the NC358 21k_75x assembly. The obtained NC358 *bz* locus is 289,103
515 bp in length (chr9:11625031..11914133), which is 50 kb longer than that of the W22 *bz* locus (238,141
516 bp). Similarly, the 2-kb flanking sequences of the NC358 21k_75x *bz* locus were used to locate the *bz*
517 locus coordinates in the other NC358 assemblies.

518 The *zein* sequence was downloaded from NCBI (AF031569.1) and the *Rp1-D* from MaizeGDB
519 (AC152495.1_FG002). The same method as described for the *bz* locus was used to identify coordinates in
520 the NC358 assemblies based on blast results using 2-kb flanking sequences.

521 Data availability

522 PacBio and Illumina sequencing reads for the NC358 line used in this study are available with EBI
523 Biosample ID ERSXXXXXXX. All code developed for this study is available on GitHub:
524 https://github.com/HuffordLab/Maize_NC358.

525 ACKNOWLEDGMENTS

526 This work was supported by NSF Plant Genome Research Program grant IOS-1744001 to RKD, DW, and
527 MBH and grant IOS-1546727 to CNH, USDA ARS 5030-21000-068-00D to MBH and MW, and USDA
528 ARS 58-8062-2100-044 to DW. BPW, SK, and AMP were supported by the Intramural Research
529 Program of the National Human Genome Research Institute. We wish to acknowledge Jonathan Gent for
530 helpful discussion on repeat space analyses.

531 AUTOHR CONTRIBUTIONS

532 RKD, CNH, MBH, and DW conceived the study. AF, CSC, SO, and AS assembled the genomes.
533 SO, JL, KMC, AF, AS, JS, VL, NM, AMG, XW, CSC, DEH, SP, SS, KF, MW, BPW, SK, AMP,
534 and BH collected data and conducted the analyses. SO, JL, AF, AS, VL, RKD, CNH, MBH, DW
535 wrote the manuscript. All authors read and approved the final manuscript.

536 COMPETING INTERESTS STATEMENT

537 The authors declare that they have no competing interests.

538 REFERENCES

- 539 1. Adams, M. D. *et al.* The genome sequence of *Drosophila melanogaster*. *Science* **287**, 2185–2195
540 (2000).
- 541 2. Lander, E. S. *et al.* Initial sequencing and analysis of the human genome. *Nature* **409**, 860–921
542 (2001).
- 543 3. The Arabidopsis Genome Initiative. Analysis of the genome sequence of the flowering plant
544 *Arabidopsis thaliana*. *Nature* **408**, 796–815 (2000).
- 545 4. Swarbreck, D. *et al.* The Arabidopsis Information Resource (TAIR): gene structure and function
546 annotation. *Nucleic Acids Res.* **36**, D1009–14 (2008).
- 547 5. International Wheat Genome Sequencing Consortium (IWGSC) *et al.* Shifting the limits in wheat
548 research and breeding using a fully annotated reference genome. *Science* **361**, (2018).
- 549 6. Alkan, C., Sajjadian, S. & Eichler, E. E. Limitations of next-generation genome sequence assembly.
550 *Nat. Methods* **8**, 61–65 (2011).
- 551 7. Ou, S., Chen, J. & Jiang, N. Assessing genome assembly quality using the LTR Assembly Index
552 (LAI). *Nucleic Acids Research* **46**, e126 (2018).
- 553 8. Miga, K. H. *et al.* Telomere-to-telomere assembly of a complete human X chromosome. *bioRxiv*
554 735928 (2019). doi:10.1101/735928
- 555 9. Chia, J.-M. *et al.* Maize HapMap2 identifies extant variation from a genome in flux. *Nat. Genet.* **44**,
556 803–807 (2012).
- 557 10. Jiao, Y. *et al.* Improved maize reference genome with single-molecule technologies. *Nature* **546**,
558 524–527 (2017).
- 559 11. Chin, C.-S. *et al.* Phased diploid genome assembly with single-molecule real-time sequencing. *Nat.*
560 *Methods* **13**, 1050–1054 (2016).

- 561 12. Koren, S. *et al.* Canu: scalable and accurate long-read assembly via adaptive k-mer weighting and
562 repeat separation. *Genome Res.* **27**, 722–736 (2017).
- 563 13. Yan, J. *et al.* Genetic characterization and linkage disequilibrium estimation of a global maize
564 collection using SNP markers. *PLoS One* **4**, e8451 (2009).
- 565 14. Lu, F. *et al.* High-resolution genetic mapping of maize pan-genome sequence anchors. *Nat.*
566 *Commun.* **6**, 6914 (2015).
- 567 15. Simão, F. A., Waterhouse, R. M., Ioannidis, P., Kriventseva, E. V. & Zdobnov, E. M. BUSCO:
568 assessing genome assembly and annotation completeness with single-copy orthologs. *Bioinformatics*
569 **31**, 3210–3212 (2015).
- 570 16. Zook, J. M. *et al.* Extensive sequencing of seven human genomes to characterize benchmark
571 reference materials. *Scientific Data* 160025 (2016).
- 572 17. Collins, N. *et al.* Molecular characterization of the maize Rp1-D rust resistance haplotype and its
573 mutants. *Plant Cell* **11**, 1365–1376 (1999).
- 574 18. Song, R., Llaca, V., Linton, E. & Messing, J. Sequence, regulation, and evolution of the maize 22-
575 kD alpha zein gene family. *Genome Res.* **11**, 1817–1825 (2001).
- 576 19. Dooner, H. K. & He, L. Maize genome structure variation: interplay between retrotransposon
577 polymorphisms and genic recombination. *Plant Cell* **20**, 249–258 (2008).
- 578 20. Jin, W. *et al.* Maize centromeres: organization and functional adaptation in the genetic background
579 of oat. *Plant Cell* **16**, 571–581 (2004).
- 580 21. Gent, J. I., Wang, N. & Dawe, R. K. Stable centromere positioning in diverse sequence contexts of
581 complex and satellite centromeres of maize and wild relatives. *Genome Biol.* **18**, 121 (2017).
- 582 22. Santos-Serejo, J. A., Gardingo, J. R., Mondin, M. & Aguiar-Precin, M. L. R. Alterations in
583 Heterochromatic Knobs in Maize Callus Culture by Breakage-Fusion-Bridge Cycle and Unequal
584 Crossing Over. *Cytogenet. Genome Res.* **154**, 107–118 (2018).
- 585 23. Doyle, J. J. & Doyle, J. L. *A rapid DNA isolation procedure for small quantities of fresh leaf tissue.*
586 (1987).
- 587 24. Hufnagel, D. E., Hufford, M. B. & Seetharam, A. S. SequelQC: Analyzing PacBio Sequel Raw
588 Sequence Quality. *bioRxiv* 611814 (2019). doi:10.1101/611814
- 589 25. Deschamps, S. *et al.* A chromosome-scale assembly of the sorghum genome using nanopore
590 sequencing and optical mapping. *Nat. Commun.* **9**, 4844 (2018).
- 591 26. Chaisson, M. J. & Tesler, G. Mapping single molecule sequencing reads using basic local alignment
592 with successive refinement (BLASR): application and theory. *BMC Bioinformatics* **13**, 238 (2012).
- 593 27. Li, H. Minimap2: pairwise alignment for nucleotide sequences. *Bioinformatics* **34**, 3094–3100
594 (2018).

- 595 28. Walker, B. J. *et al.* Pilon: an integrated tool for comprehensive microbial variant detection and
596 genome assembly improvement. *PLoS One* **9**, e112963 (2014).
- 597 29. Tang, H. *et al.* ALLMAPS: robust scaffold ordering based on multiple maps. *Genome Biol.* **16**, 3
598 (2015).
- 599 30. Kim, D., Paggi, J. M., Park, C., Bennett, C. & Salzberg, S. L. Graph-based genome alignment and
600 genotyping with HISAT2 and HISAT-genotype. *Nat. Biotechnol.* **37**, 907–915 (2019).
- 601 31. Seetharam, A. *et al.* *ISUgenomics/bioinformatics-workbook: 2019-10-11 Release of the*
602 *Bioinformatics Workbook*. (2019). doi:10.5281/zenodo.3482894
- 603 32. Smit, A. F. A., Hubley, R. & Green, P. RepeatMasker Open-4.0. 2013--2015. (2015).
- 604 33. Schnable, P. S. *et al.* The B73 maize genome: complexity, diversity, and dynamics. *Science* **326**,
605 1112–1115 (2009).
- 606 34. Campbell, M. S., Holt, C., Moore, B. & Yandell, M. Genome annotation and curation using
607 MAKER and MAKER-P. *Curr. Protoc. Bioinformatics* **48**, 4–11 (2014).
- 608 35. Stanke, M. *et al.* AUGUSTUS: ab initio prediction of alternative transcripts. *Nucleic Acids Res.* **34**,
609 W435–9 (2006).
- 610 36. Salamov, A. & Solovyev, V. Fgenesh multiple gene prediction program. (1998).
- 611 37. Dobin, A. *et al.* STAR: ultrafast universal RNA-seq aligner. *Bioinformatics* **29**, 15–21 (2013).
- 612 38. Li, H. *et al.* The Sequence Alignment/Map format and SAMtools. *Bioinformatics* **25**, 2078–2079
613 (2009).
- 614 39. Quinlan, A. R. & Hall, I. M. BEDTools: a flexible suite of utilities for comparing genomic features.
615 *Bioinformatics* **26**, 841–842 (2010).
- 616 40. Zhang, R.-G., Wang, Z.-X., Ou, S. & Li, G.-Y. TESorter: lineage-level classification of transposable
617 elements using conserved protein domains. *bioRxiv* 800177 (2019). doi:10.1101/800177
- 618 41. Manchanda, N. *et al.* GenomeQC: A quality assessment tool for genome assemblies and gene
619 structure annotations. *bioRxiv* 795237 (2019). doi:10.1101/795237
- 620 42. Johnson, M. *et al.* NCBI BLAST: a better web interface. *Nucleic Acids Res.* **36**, W5–9 (2008).
- 621 43. Rice, P., Longden, I. & Bleasby, A. EMBOSS: the European Molecular Biology Open Software
622 Suite. *Trends Genet.* **16**, 276–277 (2000).
- 623 44. Mistry, J., Finn, R. D., Eddy, S. R., Bateman, A. & Punta, M. Challenges in homology search:
624 HMMER3 and convergent evolution of coiled-coil regions. *Nucleic Acids Res.* **41**, e121 (2013).
- 625 45. Ou, S. & Jiang, N. LTR_retriever: A Highly Accurate and Sensitive Program for Identification of
626 Long Terminal Repeat Retrotransposons. *Plant Physiol.* **176**, 1410–1422 (2018).
- 627 46. Ou, S. *et al.* Benchmarking Transposable Element Annotation Methods for Creation of a
628 Streamlined, Comprehensive Pipeline. *bioRxiv* 657890 (2019). doi:10.1101/657890

- 629 47. Hirsch, C. N. *et al.* Draft Assembly of Elite Inbred Line PH207 Provides Insights into Genomic and
630 Transcriptome Diversity in Maize. *Plant Cell* **28**, 2700–2714 (2016).
- 631 48. Xin, M. *et al.* Dynamic expression of imprinted genes associates with maternally controlled nutrient
632 allocation during maize endosperm development. *Plant Cell* **25**, 3212–3227 (2013).
- 633 49. Yang, N. *et al.* Contributions of *Zea mays* subspecies *mexicana* haplotypes to modern maize. *Nature*
634 *Communications* **8**, (2017).
- 635 50. Springer, N. M. *et al.* The maize W22 genome provides a foundation for functional genomics and
636 transposon biology. *Nat. Genet.* **50**, 1282–1288 (2018).
- 637 51. Marçais, G. & Kingsford, C. A fast, lock-free approach for efficient parallel counting of occurrences
638 of k-mers. *Bioinformatics* **27**, 764–770 (2011).
- 639 52. Albert, P. S., Gao, Z., Danilova, T. V. & Birchler, J. A. Diversity of chromosomal karyotypes in
640 maize and its relatives. *Cytogenet. Genome Res.* **129**, 6–16 (2010).

641 FIGURE LEGENDS

642 **Figure 1.** Assembly of NC358 using various read lengths and coverage. (A) Hybrid scaffolding using the
643 Bionano optical map. A 199-Mb scaffold from chromosome 5 is shown. Grey areas on the chromosome
644 cartoon represent the 199-Mb scaffold; the white area is the remaining 23-Mb scaffold in chromosome 5;
645 the red dot is the centromere. Green tracts represent scaffolded sequences, and blue tracts show the
646 contigs that comprise this scaffold with contigs jittered across three levels. (B) Contig NG(x). (C)
647 Scaffold NG(x). (D) BUSCO. (E) The number of conflicts between Bionano contigs and sequence contigs
648 and the number of contigs of each assembly. (F) Regional LAI values estimated based on 3-Mb windows
649 with 300-kb steps. (G) Unique mapping rate of RNA-seq libraries. Each dot represents an RNA-seq
650 library. (H) CPU core hours required for Falcon correction and Canu assembly. (I) Bionano optical map
651 inconsistency. Deletions and insertions are cases where sequences are shorter or longer than the size
652 estimated by the optical map, respectively.

653

654 **Figure 2.** Assembly of repetitive components in the NC358 genome. (A) The assembled size of the 180-
655 bp knob repeat, the knob TR-1 element, the chromosome 6 NOR region, CentC arrays, and subtelomere
656 arrays in each of the NC358 assemblies. (B) Length distribution of LTR retrotransposons longer than 26
657 kb. Each dot represents an annotated sequence. (D) Telomere 7-mer counts in telomere regions of NC358
658 assemblies. Assembly of (C) LTR retrotransposons, (E) CentC arrays, (F) the chromosome 6 NOR region,
659 (G) the *Rp1-D* and *zein* tandem gene arrays, and (H) two example knobs in each of the NC358 assemblies.

660 The NC358 Bionano optical map was used to estimate the size of these components. Ngap, estimated gap
661 size.

662 TABLE

663 **Table 1.** Summary statistics for NC358 assemblies.

Experiment	21k_20x	21k_30x	21k_40x	21k_50x	21k_60x	21k_75x	11k_50x	16k_50x
Raw reads (Gb)	45.62	68.16	91.01	113.89	136.80	171.08	113.63	113.60
Raw coverage	20x	30x	40x	50x	60x	75x	50x	50x
Max read length (kb)	89.6	103.3	103.3	103.3	103.3	103.3	88.3	69.8
Raw read N25 (kb)	30.1	30.1	30.1	30.1	30.1	30.1	14.5	21.6
Raw read N50 (kb)	21.2	21.2	21.2	21.2	21.2	21.2	11.1	16.8
Corrected reads (Gb)	25.11	48.13	66.05	82.96	88.93	100.90	79.26	80.22
Corrected coverage	11x	21x	29x	37x	39x	44x	35x	35x
Corrected read N50 (kb)	18.42	17.13	17.10	17.25	18.80	20.05	10.37	14.48
Contig number	10,563	2,015	641	407	360	327	5,683	1,036
Contig total (Gb)	1.60	2.11	2.12	2.12	2.13	2.13	2.10	2.12
Longest contig (Mb)	1.06	11.50	47.89	76.00	79.68	78.40	4.37	21.45
Contig N50 (Mb)	0.18	1.82	7.48	16.27	22.12	24.54	0.56	4.24
Longest scaffold (Mb)	198.5	198.7	237.1	237.2	237.1	237.3	205.4	237.6
Scaffold N50 (Mb)	95.3	96.9	99.2	98.5	99.4	99.2	98.5	99.4
Assembled (%) ^a	70.4%	92.8%	93.3%	93.3%	93.7%	93.7%	92.4%	93.2%
Assembly gaps (%)	24.50%	0.90%	0.43%	0.34%	0.31%	0.31%	2.01%	0.48%
Effective assembly size (Gb) ^b	1.33	1.67	1.70	1.72	1.74	1.75	1.68	1.70
Optical map conflict ^c	594	125	56	31	22	21	386	107
Complete BUSCOs ^d	68.0%	95.5%	96.5%	96.4%	96.2%	96.3%	95.7%	96.7%
LTR Assembly Index (LAI)	12.2	19.8	20.4	20.2	20.4	20.6	19.1	21.0
Falcon CPU hour	1,563	4,162	6,363	10,693	12,386	32,950	9,721	9,224
Falcon RAM (Gb)	75	75	75	75	75	75	75	75
Canu CPU hour	1,860	4,036	5,959	7,914	8,849	11,520	6,400	7,174
Canu RAM (Gb)	61	112	149	177	201	120	183	174

664 ^aCalculated based on total contig size and the estimated genome size of 2.2724 Gb. ^bSum of unique 150-
665 mers. ^cThe optical map was generated using the Direct Label and Stain (DLS) approach with enzyme
666 DLE-1. ^dPilon-polished assemblies were used to calculate BUSCO.